# A new higher-resolution multi-trace seismic discontinuity attribute based on a Dynamic Time Warping algorithm

I.I. Priezzhev[1], D.A. Danko[1], U. Strecker[2] and P.C.H. Veeken[3*]


## Abstract

A new machine-learning approach based on a Dynamic Time Warping (DTW) algorithm is introduced to detect faults and fractures in 3D seismic data from an unconventional resource play in Eastern Cis- Caucasia (Russia). This novel approach allows for better edge detection in seismic amplitude volumes because it employs a detailed comparison of two neighbouring traces to detect discontinuity via a minimal horizontal distance. For benchmarking purposes the proposed DTW method is compared to a widely used multi-trace attribute (Variance). Subsequently, both calculated attribute cubes serve as an input for ANT-Tracking to delineate fault strike and fracture corridor trends. A comparison of results shows that better resolution and more complete fault images are obtained when the DTW method is applied.


## Introduction

Fault and fracture detection, based on mapping phase discontinuities in 3D seismic volumes, is a high priority task for petroleum industry geoscientists. Horizon or time slice analysis of multi-trace seismic attributes is not only useful for mapping stratigraphic features, such as channel margins, but is of particular interest for fault detection and mapping of fracture zones (e.g. fracture corridors) in hydrocarbon exploration and production projects. These features are important for prospecting unconventional hydrocarbon resource plays, e.g. Vaca Muerta source rocks (Curia and Veeken, 2019) and in other business domains where faulted areas play a decisive role, such as geohazard assessment or dynamic reservoir model simulations (discrete fracture networks; Buijs et al., 2019). Typically, multi-trace edge detection algorithms are applied on seismic amplitude volumes to highlight horizontal discontinuities which are interpreted as faults or subtle fractures (Priezzhev et al., 2019). In poorly noise-suppressed seismic amplitude data, false positives generated from acquisition footprint should be filtered out by factorial kriging, or excluded by directional (orthogonal decomposition) principal component analysis (Priezzhev et al., 2010). True positive edges generally appear as low-amplitude, low coherency samples on 2D cross sections and/or as lineaments associated with phase breaks on the 3D slices or seismic surfaces.

In the upstream petroleum industry many different algorithms exist for 3D seismic edge detection. The attribute list includes: coherence cube, variance cube, local angle and azimuth angle (Dalley et al., 1989; Marfurt, 2006); minimum, maximum, Gaussian curvature, and others (Flynn and Jain, 1989; Roberts, 2001; Chopra and Marfurt, 2007a); 3D curvatures; spectral decomposition (Chopra and Marfurt, 2007b, 2009), and thinned fault likelihood (Hale and Wu, 2015). However, low resolution for the resulting output volumes and maps is a common problem related to conventional fracture and fault detection technologies. Building on previous research of fracture and fault detection techniques via detailed seismic data analysis (Priezzhev and Scollard, 2012; Priezzhev and Scollard, 2013), we propose to use the Dynamic Time Warping (DTW) algorithm (Sakoe and Chiba, 1978; Juang, 1984) to determine the displacement and discontinuity between two seismic traces at high resolution. In time series or trace analysis, dynamic time warping (DTW) provides a means for measuring similarity between two temporal sequences, which may vary in speed. This machine learning algorithm has proved useful in speech recognition for example (e.g. Nakagawa and Nakanishi 1988). The DTW approach offers additional detection capability for subtle fractures or small-throw faults. The output of this new seismic discontinuity analysis method is called the 'DTW edge detection cube'. The better resolution is achieved by the horizontal base distance of its offset, i.e. the distance between the two seismic traces (cf Priezzhev et al., 2019a; Priezzhev et al., 2019b). The improvement is readily apparent in comparison to the calculation of other multi-trace fault detection methods, where a moving window is used instead. The horizontal offset base is considered as the size of the computation window that defines the resolution of these methods. In the DTW process the vertical resolution of the proposed edge detection technique is also improved by the search engine, because a different correlation is made from trace sample to trace sample, as described in more detail below.

[1] Gubkin Russian State University of Oil and Gas | [2] Wintershall Dea GmbH | [3] Geops Consultancy
[*] Corresponding author, E-mail: pveeken@hotmail.com
DOI: 10.3997/1365-2397.fb2020025

## Discontinuity and edge detection method

Let us assume that there are two seismic traces, with elements $\{s_1^1, s_2^1, s_3^1, \ldots, s_N^1\}$ and $\{s_1^2, s_2^2, s_3^2, \ldots, s_N^2\}$, where the upper index is the trace number and the lower index is the sample number. Let us denote the DTW matrix as a matrix of squared differences between all elements of the two curves $S_{ij} = (s_i^1 - s_j^2)^2$ or, alternatively, the absolute value of the difference $S_{ij} = \left| s_i^1 - s_j^2 \right|$. It is necessary to find a path $r$ through this DTW matrix from the first element (1,1) to the final element at (N, N) with the minimum sum of elements of this matrix according to equation 1 and as shown in Figure 1A.

$$r = \sum_{ij} S_{ij} \rightarrow min \qquad (1)$$

The following boundary conditions must be observed: a.) continuity between elements in the path where there are no gaps and all the elements are adjacent, b.) the concept of monotonousness means the indices (i, j) of elements steadily increase, i.e. they must not decrease.

Figure 1 (B and C) demonstrate the comparison of the Euclidean and DTW matching approach for adjacent curves and in our case two adjacent seismic traces are shown. Figure 1B demonstrates how the shift between two traces can clearly be determined if DTW matching is applied. In the case when Euclidean matching is selected (Figure 1C), as is usually the case in conventional approaches, it is very difficult to find exact shifts.

The algorithm can be used in a moving window across the seismic volume with the defined vertical size and comprising 3 x 3 traces. The DTW matching algorithm can be applied for two traces in this window; one of these is to be the central trace and the second one can be any other trace in the window. The shift is estimated only for the central sample in the moving window whereby the vertical window size should be long enough to estimate this shift. The shift according to the DTW algorithm will be determined as the difference in indexes in units of the number of samples of integer value. To get a more precise value of the time (or depth) shift, it is necessary to apply interpolation for the DTW path or perform an averaging calculation for the nearest shifts to the central sample of the moving window. In this case, the resulting shift will be proportional to the dip angle from the side of the second trace. Another variant is to calculate a maximum shift from all traces around the central trace in the moving window.

Eight traces are used to calculate shifts with a central trace in the 3D edge detection approach (Figure 2). Averaging of the computed shifts stabilizes the results. The vertical computation window size is an important parameter because it allows us to calculate the shift more precisely. Optional interpolation determines the exact shift in the middle point of the window. Moreover, the DTW results are expressed as integer values. The method of vertical averaging plus averaging for all traces works much better than the vertical interpolation of the maximum value. The method avoids the subtle negative averaging effect of the more traditional moving window schemes.

The DTW method eliminates the normal trend of the reflection surface if we sum up the opposite (from different sides of the central trace) shifts with different signs. The scheme of the normal trend removal is shown in Figure 2B. This feature helps us to image faults on steeply plunging structures, which is not possible when applying conventional techniques only.

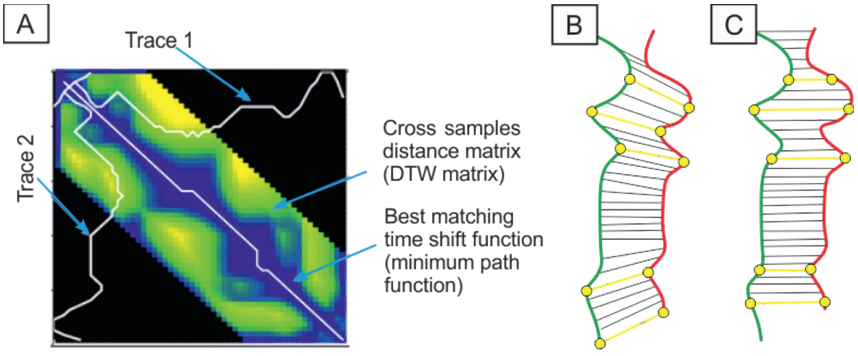


**Figure 1** (A) Graphic representation of DTW matrix allowing comparison of two seismic traces based on a cross-sample distance matrix and definition of the best-matching time-shift function. Comparison of two traces: (B) – using DTW matching and (C) – Euclidean matching. Note that the DTW allows for correlation with different directionalities.

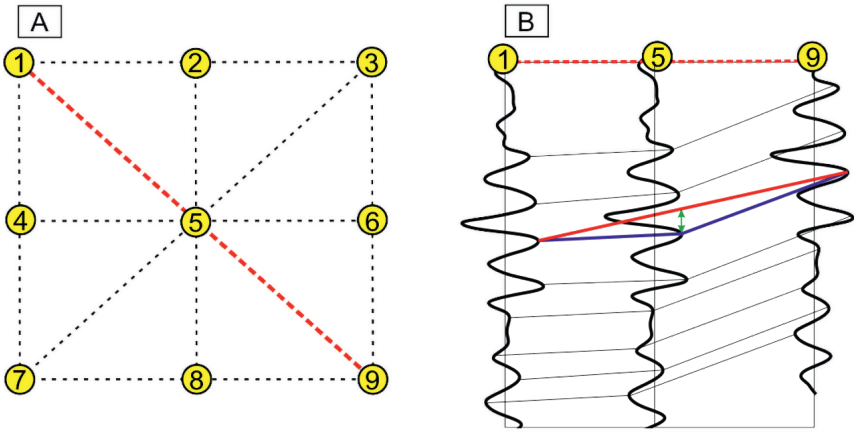


**Figure 2** (A) 3 x 3 traces moving window calculation shifts scheme. The shifts are calculated in directions 1-5, 2-5, 3-5, 4-5, 6-5, 7-5, 8-5 and 9-5. (B) Removing normal structure trend scheme. Red line shows the normal trend. The difference between the red and blue line is the calculation shift at the central trace without the trend.

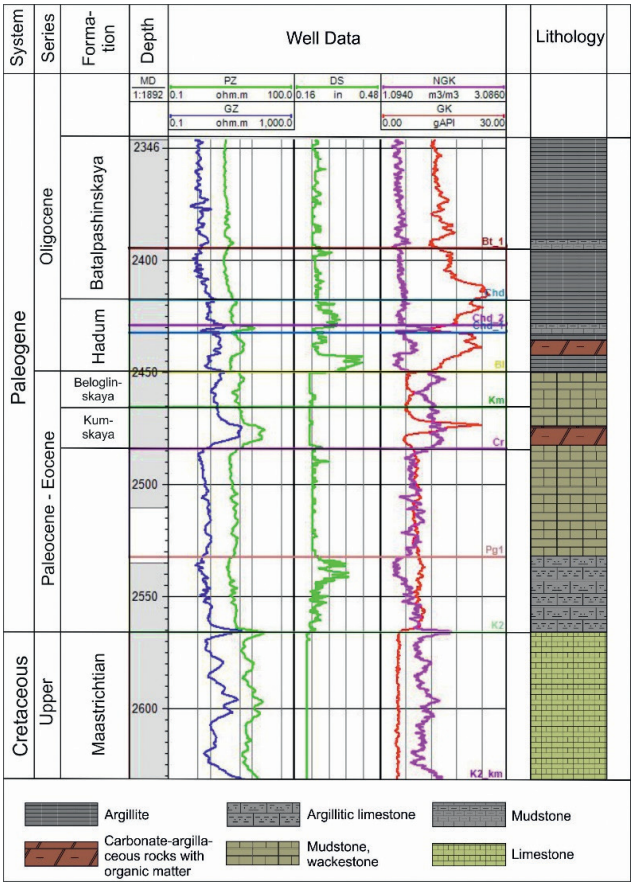


**Figure 3** Chrono-stratigraphic column, well log data and lithological classification of Eastern Cis-Caucasia region, showing target intervals (Paleocene-Eocene and Oligocene series). The reservoir properties of all intervals are associated with a fractured type of porosity that increases the permeability and flow characteristics.

## Application of DTW technology for fault and fracture identification

The 'DTW edge detection cube' technology was applied to identify faults and fractures in an oil field in the Russian onshore Eastern Cis-Caucasia region. The input data is a 3D post-stack time-migrated seismic survey cube that was acquired in 2018. To test the feasibility of applying DTW technology, the 3D survey was cropped to 190 inlines by 160 crosslines and the two-way travel time interval was cut approximately at the Top Oligocene Batalpashinskaya Fm and the Base Maastrichtian (around 1000 ms with 2 ms sample rate). The bin size of seismic data is 25 x 25 m, mean fold (or coverage) is 65 with maximum offsets reaching 4000 m. There are 7 wells available in a historic well repository for the study area. One well with a more complex logging suite and detailed core measurements was drilled at the beginning of 2019. The target intervals are rocks of the Oligocene and Paleocene-Eocene age (organic shales, argillite, mudstone, wackestone, carbonates rocks and mixed rocks). The well log and lithostratigraphic column is shown in Figure 3.

The peculiarity of this oil field is that the reservoir properties of all target intervals are associated with a dual porosity, i.e. a fracture-connected porosity system. Therefore, detailed fault and fracture identification using seismic data is considered one of the most important aims to predict: 1) prospective zones (e.g. Ma and Holdich, 2016; Vernik, 2016), 2) build a geomechanical model, 3) drill horizontal wells and 4) conduct hydraulic fracturing (e.g. Zoback, 2007).

The main approach for predicting fracture zones from seismic data is to calculate different multi trace 'geometric' attributes such as: curvature, variance, chaos, fault indicator, dip or slope, azimuth, continuity, chaos measure, diffraction energy etc. (cf Barnes, 2016; Beller et al., 2019). One of the most popular and useful tools for identifying and interpreting faults is ANT-tracking technology (Skov et al., 2003). It represents the machine learning part of our workflow. The technology imitates the behaviour of ants in nature and how they use pheromones markers for food searching. Virtual ants are used to look for fault zones based on discontinuity of the seismic data. In addition, illegal steps can be defined to liberalize the ants' search criteria and extend existing discontinuities along trend to connect separate patches of the same fault. The result is an attribute volume that shows very sharp and detailed edges interpreted as fault zones. To enhance major faults, three calculated attributes (Variance, Chaos or dip) can be used in the standard workflow. Variance estimates the local signal variance and Chaos measures the 'lack of organization' in the dip and azimuth estimation method. In this case study, the ANT-tracking workflow was modified by replacing the required standard input attribute (Variance, Dip or Chaos) with a DTW edge-detected volume (Figure 4). The DTW search engine allows different directions to be used in the similarity and trace comparisons.

Figure 5 shows the result of fault interpretation using variance cube seismic attributes. Figure 6 shows the results of the newly proposed DTW edge detection cube technology using the same dataset as in the previous case. It is clearly seen that the result contains more detail and is informative, especially in the northern and southern parts of the studied area (Figure 7).

Fractures occur when brittle rocks exceed the yield strength, but the relationship between open cracks and various measures of curvature is quite complex as it depends on lithology, previous faults and cracks, paleo-stress direction, pore pressure and current stress mode (i.e. critically stressed fractures). Nevertheless, maps of different geometrical attributes obtained from seismic data can provide an accurate map of present-day

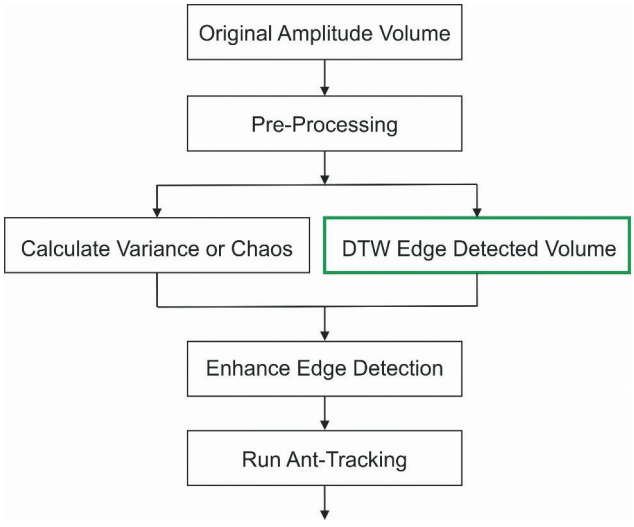


**Figure 4** ANT-Tracking workflow with DTW technology added.

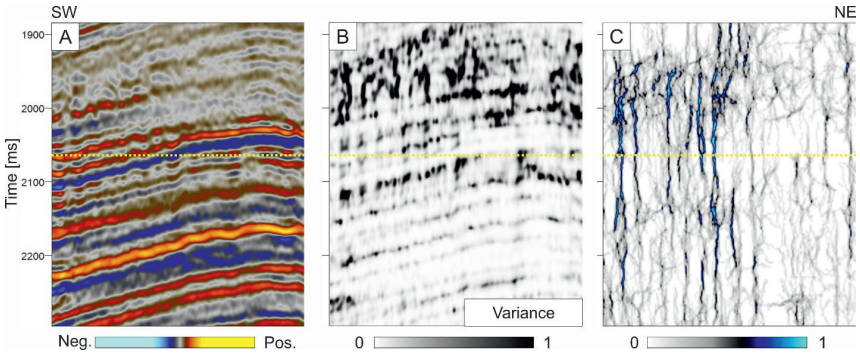


**Figure 5** Cross sections: (A) Input seismic cube. (B) Variance cube. (C) Ant-Tracking with variance as input.

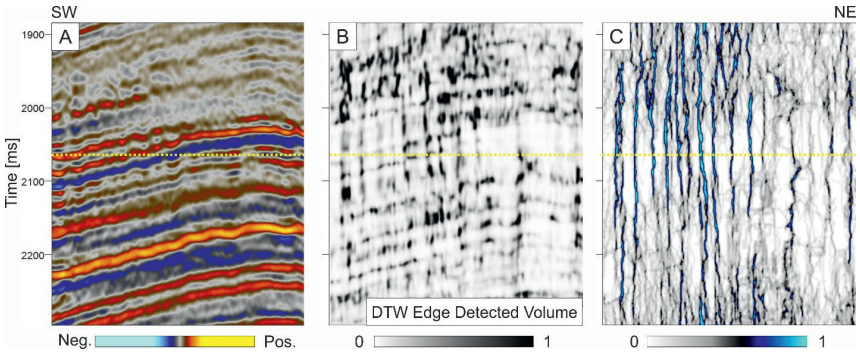


**Figure 6** Cross sections: (A) Input seismic cube. (B) DTW edge cube. (C) Ant-Tracking with DTW edge as input.

subsurface structure. If the deformation was simple and the current stress mode has not changed since the structural deformation, such maps can be used to predict open (i.e. critically stressed) fractures (Chopra and Marfurt, 2007). However, the goal of predicting fracture zones in seismic data is limited by seismic resolution both vertically and laterally. The identified structural anomalies in the seismic wavefield can generally be associated with fault zones, but moving to a more detailed scale (i.e. to fracture scale) requires the use of high resolution well log and core data.

Figure 7 shows a zoom-in rectangle of the area around a recently drilled well. There are no fault anomalies on the ANT-track time slice calculated using the Variance attribute, but the time slice result, based on the proposed 'DTW edge detection cube' attribute cube, features a newly imaged fault anomaly passing directly through the well control. Note also the amplitude difference of the mapped edge. In this well, cross-dipole acoustic logging, full-bore formation micro imager data and a detailed description of the core material are available. A study of the shear wave azimuthal anisotropy showed that there are three intervals with sub-vertical fractures and these intervals are confirmed by core data analysis. Figure 8 illustrates a comparison of the anisotropy intervals from the well logging with the core data. Sub-vertical cracks are clearly visible on the core samples.

A comparison of the results of fault identification based on the proposed DTW technology and the anisotropy intervals extracted from well data are shown in Figure 9. The well in depth has been calibrated to the seismic data in time with a good tie, giving confidence in the time-depth curve. The ANT-tracking fault anomaly obtained using the DTW method shows a clear sub-vertical fault, which is confirmed by core and logging measurements. Therefore, the presented DTW method has been

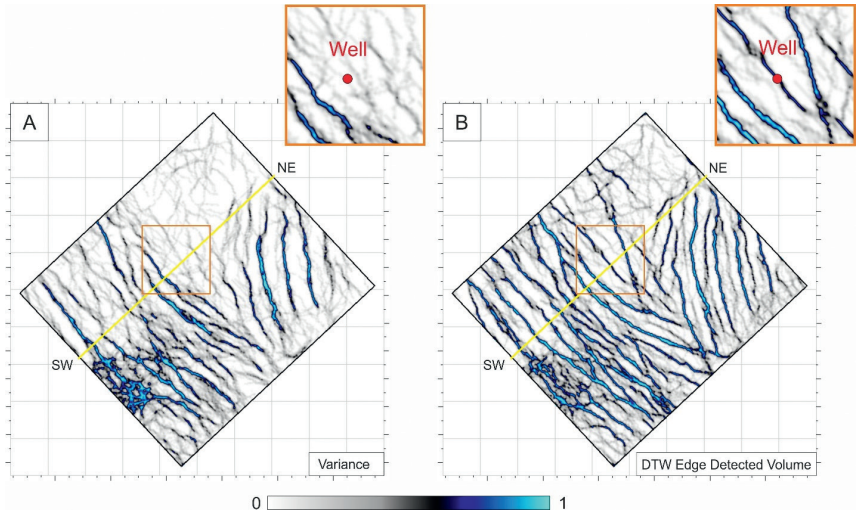


**Figure 7** Time slices of the ANT-Tracking calculated results based on Variance attribute (A) and based on the proposed 'DTW edge detection cube' attribute (B). In the north and south areas the DTW result demonstrates better detection than Variance. An orange rectangle shows a zoom-in of the area around the control well (red dot). The mapped fault was penetrated by the well trajectory and a fracture zone was confirmed despite the possible time migration inaccuracy.

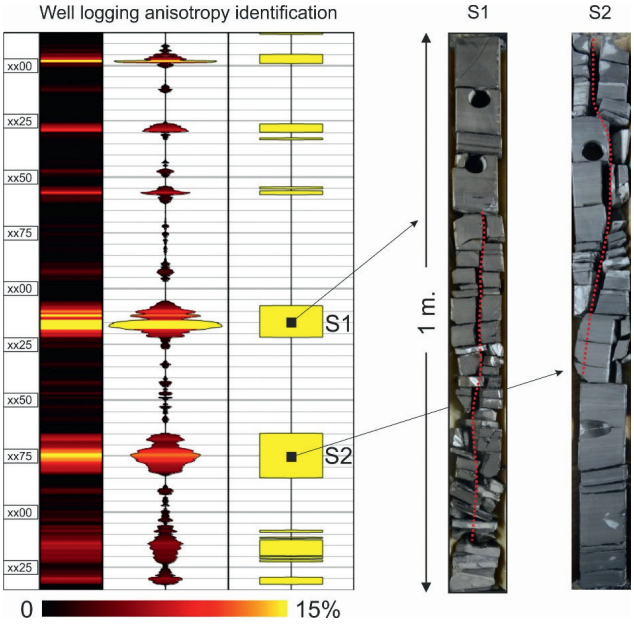


**Figure 8** Comparison of cross-dipole acoustic logging interpretation at the control well exhibiting intervals with pronounced anisotropy (yellow blocks) alongside the core data. Sub-vertical fractures (red dotted line) are clearly visible on the core samples.

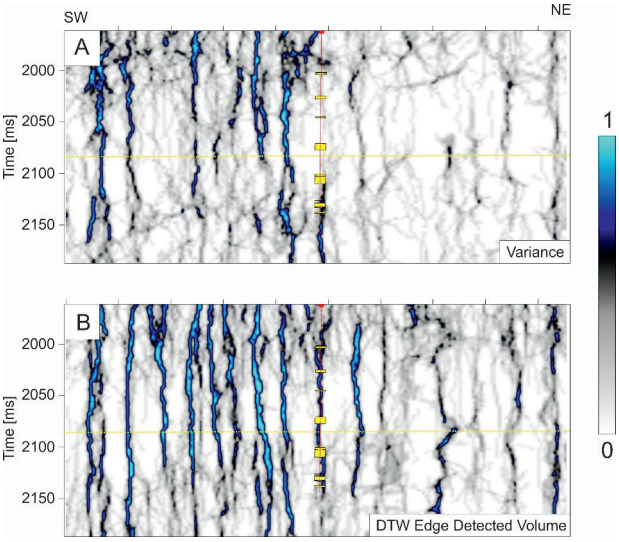


**Figure 9** A comparison of the result of fault identification based on the proposed DTW technology and the anisotropy intervals extracted from well data and core analysis (yellow blocks). (A) – a cross section via ANT-Tracking in a volume that used a variance cube like input, (B) – a cross section via ANT-Tracking cube that used DTW edge detection cube as input.

selected for creating a more accurate fault block model in the continuing field operations.

It should be mentioned that the presented ANT-tracking fault models (Variance and DTW) were not used for predicting the optimal well-head position and the results of the drilled well (Figure 7). The well was drilled after the DTW workflow was done. Therefore, it enables testing of the DTW algorithm in the study area, i.e. it serves here as a blind test of the applied technique. After comparison with well logs and core data analysis the ANT-tracking model with 'DTW edge detection cube' was used for: 1) planning further drilling, 2) control of the horizontal

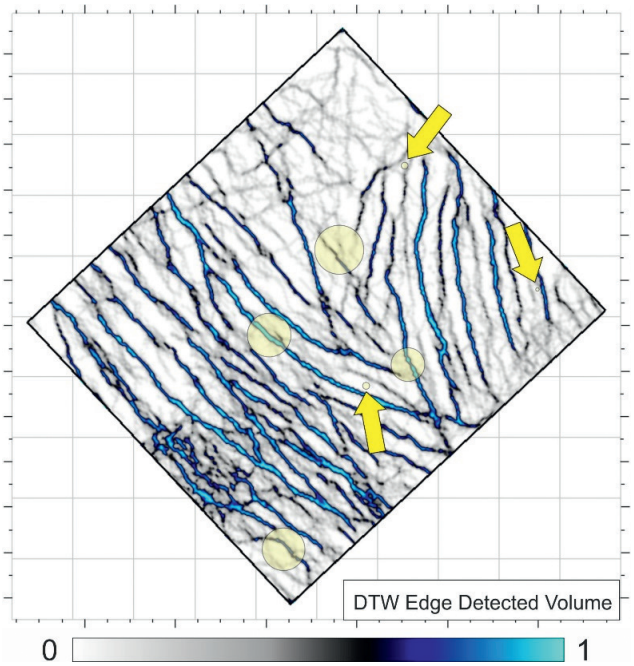


**Figure 10** Time slice of the ANT-Tracking calculated results based on the proposed 'DTW edge detection cube' attribute. The size of the circles is proportional to the best year's production. Note that the larger circles correlate with fault and fracture anomalies, whereas poor productivity wells do not (yellow arrows).

cluster of wells and 3) the design of hydraulic fracturing in the target formations.

A criterion for the reliability of identified faults and fractures zones is to look for a relationship with the drilling results and production performance (cf Buijs et al., 2019; Curia and Veeken 2019). The DWT results for the whole survey are summarized in Figure 10. The yellow circles show the productivity of the wells in the studied field. The size of the circles is proportional to the best year's production. There is a correlation between the size of the circles and the ANT-tracking fault anomalies obtained from the DTW attribute volume, whereas a prominent fault trace is absent for much of the interval producing from fractures in the seismic variance section. This observation is important subsurface imaging detail added by DTW edge detection as it allows identification of the mapped seismic anomalies as decompression zones coinciding with the presence of open fractures. We reason that this decrease in attribute contrast either indicates less fault slip, advanced cementation or possibly represents low-probability faults that could be attributed to weak fault artefacts, sometimes associated with the application of ANT-Tracking technology in the presence of linear noise.

## Conclusions

The new, multi-trace 3D DTW edge detection seismic attribute is compared to the widely used variance attribute on a dataset from Eastern Cis-Caucasian region in order to detect faulted and fractured areas in the seismic volume. Results are summarized as follows:

- 'Sweet spots' have been delineated over the studied Tertiary target interval in these unconventional resources. The reservoirs do show a strong fracture assisted porosity/permeability behaviour.

- The comparison of edge detection methods (Dynamic Time Warping versus conventional Euclidian Variance ANT-Tracking) demonstrates that the proposed 3D discontinuity attribute has a better resolution than the conventional one.
- The better resolution of the DTW edge detection attribute is the result of the smaller horizontal base distance between the two seismic traces when compared to other correlation methods that use a moving computation window. It is the horizontal offset base and the size of the investigation window that warrant a better resolution of this newly applied analytical method.
- Application of the DTW matching approach allows estimation of time shifts between two traces in a very accurate and robust manner. The results on the 3D seismic cross sections look more continuous and after ANT-Tracking show a better resolution than standard methods.
- The method was successfully applied on a dataset from the Pre-Caucasian Basin. The presence of open fracture sets was confirmed by data from later drilled wells.

## Acknowledgements

The authors gratefully acknowledge the Department of Subsoil Use in the North Caucasus Federal District (Kavkaznedra) for permission to use their seismic and well data. We would also like to thank our colleagues from departments of Exploration Geophysics, Geophysical Well Logging and Lithology of Gubkin Russian State University of Oil and Gas for their contribution and constructive discussions.

This research has been supported by Natural Resources Ministry and Ecology and Federal Agency on Subsoil Use of Russian Federation (government contract #01-17-UVS). The presented results have been generated using ANT-Tracking technology provided by Petrel Software (Schlumberger).

## References

Barnes, A.E. [2016]. *Handbook of poststack seismic attributes*. SEG, Geophysical references series No.21.

Beller, M., Chaouch, N., Petri, V., Veeken, P., Landa, E., Kokoshin, E., Smirnov, K. and Paleari, C. [2019]. Diffraction imaging: resolving subtle seismic geo-features in the Rembrandt and Vermeer Chalk fields, Dutch offshore block F17. *81th EAGE annual Conference and Exhibition*, Extended Abstracts.

Buijs, H., Ponce, J. and Veeken, P. [2019]. Validation of flow capacity and state-of-stress models in unconventional reservoirs by the implementation of numerical models of diagnostic fracture injection tests. *The Leading Edge*, **38** (06), 306-314.

Chopra, S. and Marfurt, K.J. [2007]. Volumetric curvature attributes for fault/fracture characterization. *First Break*, **25** (7), 35–46.

Chopra, S. and Marfurt, K.J. [2007]. *Seismic attributes for prospect identification and reservoir characterization*. SEG, Geophysical references series No.11, 464.

Curia, D. and Veeken, P. [2019]. Estimating rock physical parameters using anisotropic 3D seismic data to characterise unconventional Vaca Muerta oil shale deposits in the Neuquen Basin, western Argentina. *First Break*, **38** (11).

Dalley, R.M., Gevers, E.C.A., Stampfli, G.M., Davies, D.J., Gastaldi, C.N., Ruijtenberg, P.A. and Vermeer, G.J.O. [1989]. Dip and azimuth displays for 3D seismic interpretation. *First Break*, **7** (3), 86–95.

Flynn, P.J. and Jain, K.J. [1989]. On reliable curvature estimation. *IEEE Conference on Computer Vision and Pattern Recognition*, 110-116.

Juang, B.H. [1984]. On the hidden Markov model and dynamic time warping for speech recognition #x2014; A unified view. *AT&T Bell Laboratories Technical Journal*, **63** (7), 1213-1243. doi:10.1002/j.1538-7305.1984.tb00034.x.

Ma, Y.Z. and Holditch, S.A. [2016] *Unconventional oil and gas resources handbook: evaluation and development.* Elsevier Press.

Marfurt, K.J. [2006]. Robust estimates of 3D reflector dip and azimuth. *Geophysics*, **71** (4), 29-40.

Nakagawa, S. and Nakanishi, H. [1988] Speaker-Independent English Consonant and Japanese word recognition by a stochastic Dynamic Time Warping method. *IETE Journal of Research*, **34** (1), 87-95. doi :10.1080/03772063.1988.11436710.

Priezzhev, I.I. and Scollard, A. [2012]. Fault and fracture detection based on seismic surface orthogonal decomposition. *74th EAGE Conference and Exhibition*, Extended Abstracts, W041.

Priezzhev, I.I. and Scollard, A., [2013]. Fracture detection through seismic cube orthogonal decomposition. *SEG annual conference*, Expanded Abstracts.

Priezzhev, I.I., Danko, D.A., Veeken, P.C.H., Strecker, U. and Nikiforov, A.N. [2019a]. New high-resolution discontinuity seismic attribute based on DTW (Dynamic Time Warping) algorithm. Extended abstract, *81th EAGE annual Conference and Exhibition*, Extended Abstracts.

Priezzhev, I.I., Veeken, P.C.H., Egorov, S.V. and Strecker, U. [2019b]. Application of machine learning algorithms using seismic data and well logs to predict reservoir properties. *The Leading Edge*, **38**, (12), 306-315, Doi:10.1190/tle38110306.1.

Roberts, A. [2001]. Curvature attributes and their application to 3D interpreted horizons. *First Break*, **19** (2), 85–100.

Sakoe, H. and Chiba, S. [1978]. Dynamic programming algorithm optimization for spoken word recognition. *IEEE Transactions on Acoustics, Speech, and Signal Processing*. **26** (1), 43-49. doi:10.1109/tassp.1978.1163055.

Skov, T., Pedersen, S.I., Valen, T.S., Fayemendy, P., Gronlie, A., Hansen, J.O., Hetlelid, A., Ivensen, T., Randen, T. and Sonneland, L. [2003]. Fault system analysis using a new interpretation paradigm. *65th EAGE Conference and Exhibition*, Extended Abstract.

Vernik, L. [2016]. *Seismic petrophysics in quantitative interpretation.* Investigation in Geophysics No. 18. SEG Press, Tulsa, USA.

Wu, X. and Hale, D. [2015]. Horizon volumes with interpreted constraints. *Geophysics*, **80** (2), IM21-33. Doi: 10.1190/geo2014-0212.1

Zoback, M.D. [2007]. *Reservoir geomechanics*. Cambridge Press, United Kingdom.